A Force-based Assemblability Analysis for a Robotic 3D Block Printer

*Pedro Saman Diogenes N CESARINO (Yokohama National University), Yusuke MAEDA (Yokohama National University)

1. Introduction

Assembling objects with building blocks is also considered additive manufacturing. Two of its greatest advantages are: the potential of assembling a wide range of shapes composed of multiple materials [1] and the possibility to easily disassemble an object to reuse its blocks.

Previously, a 3D block printer system was developed to assemble automatically toy brick sculptures [2]. First the object 3D CAD model is used as input and converted to a voxelized model. Then a block model is generated utilizing the "nanoblock" size parameters. Later an assembly plan is decided with the block ordering with possible subassemblies. Finally, the robot movement plan is generated to automatically build the structure in a simulated or real world scenario.

A reliable assembly plan should have some indicative of stability. In our previous study, a force-based mechanical analysis was developed to first calculate the position of every force acting in a input model and to then verify the structure static force and moment balance during and after each block insertion [3]. But to know the exact value of each friction and normal force in complex block systems would be hard. To tackle this issue, a linear programming problem was defined to search for a good force distribution in a given setting.

A metric called "capacity" was used in [4] to evaluate the assembly plan stability. This metric is defined as the difference between the maximum possible and the resultant friction force and it is calculated for each block connection. Positive capacity value means that the connection can still handle forces without breaking. Negative capacity value means that force is overflowing in that connection.

One limitation of the previous mechanical analysis [3] was that it only accepted input models with the three smallest blocks. That condition restricted much the complexity of usable objects. It also increased the 3D block printer assembly time because utilizing bigger blocks would require less overall brick insertion in the final assembly plan.

Aiming to reduce this limitation, the force-based mechanical analysis were restructured with a new force position calculation strategy to simplify it and increase the input possible block types. Also, all the experimental values necessary to the algorithm were recalculated and remeasured to improve the program output reliability.

2. Mechanical Analysis

This work was developed in MATLAB environment to make use of its optimization toolbox to solve the linear programming problem. The stability judge algorithm has three sections: the first to determine every force position in the input model and how the insertion force will be applied, the second to define the linear programming problem matrices and bounds, and the last to call the optimization function to search for a solution and give the final stability result.

2·1 Force Position

The previous strategy to define the possible force positions [3] relied on the manual definition of each of them. It was monotonous and increasingly hard to implement bigger blocks. At that time, it was decided that only the 1 by 1, 1 by 2 and 2 by 2 blocks were going to be used restricting the input 3D models and greatly increasing the time and resources needed to construct them.

The new strategy takes advantage of the geometric symmetry of the nanoblock bricks in the X and Y axis. The internal structure and top view of a 2 by 4 block can be seen in Fig. 1. A block N by M is equal to a M by N but rotated 90^{o} in the Z axis.

For each block in the input model, the algorithm automatically defines every single force that could appear and then analyzes every other block in the vicinity to determine which of the forces actually exists. Fig. 2 illustrates the force-model of a 2 by 4 brick when it is placed above other block.

Three types of force were defined when two blocks are connected. The external normal force in the Z axis appears due the physical contact when one block is above the other. The internal normal force is located in the contact points between the lower block knob and the internal walls of the upper block. The friction force appears when there is a connection between blocks in the Z axis and has its origin in the same contact points as the second normal force.

There was also defined one type of force when two

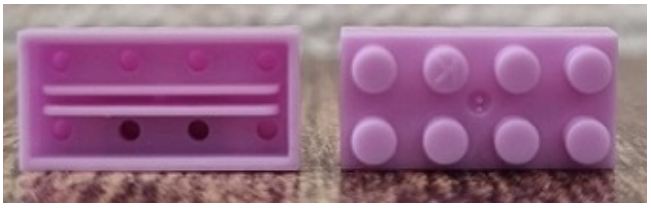

Fig. 1: Block top and bottom view of a 2 by 4 block.

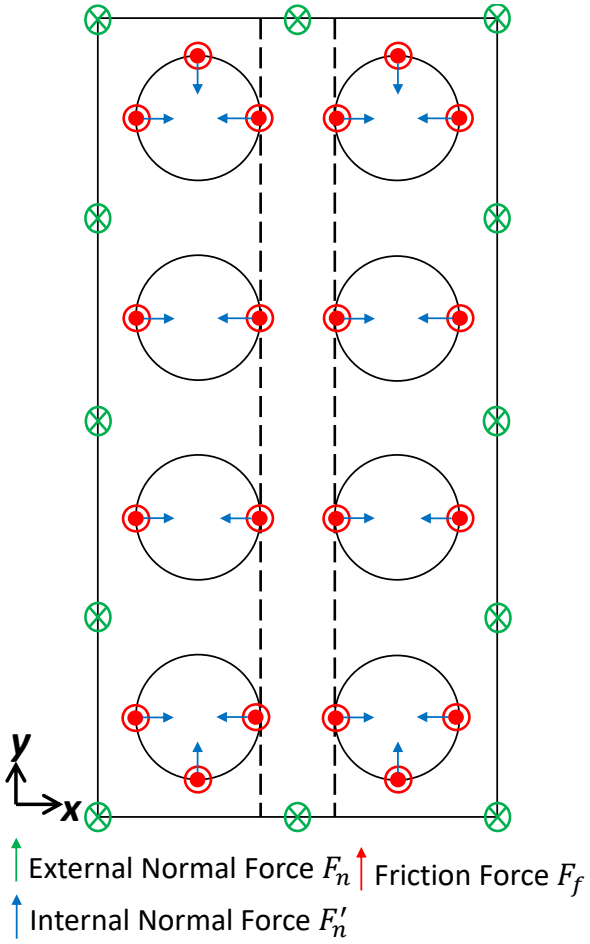

Fig. 2: Force-based model of a 2x4 block.

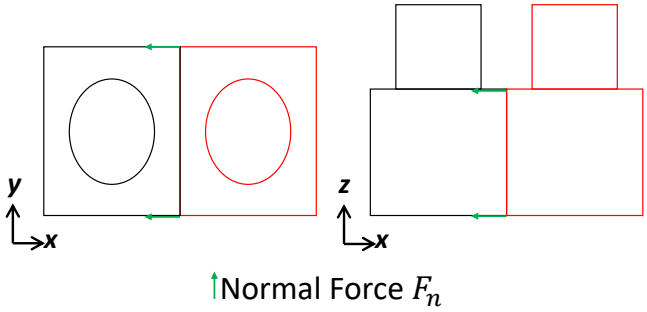

Fig. 3: Horizontal normal forces.

blocks are touching each other in the X or Y axis as shown in Fig. 3. A horizontal normal force appears in each edge of the touching surface.

The new strategy to automatically calculate the force position enabled the mechanical analysis to utilize any symmetric block from 1 by 1 to 1 by 9 and from 2 by 1 to 2 by 9. It would be possible to use more blocks, like 3 by 4 or 3 by 3, but those nanoblock types were not found and more information on them would be necessary.

Table 1: Mass experiment results.

Block type	Mass (g)
1x1	0.0380
1x2	0.0695
1x3	0.0971
1x4	0.1288
2x2	0.1266
2x4	0.2458
2x8	0.4583

2·2 Linear Programming Problem

Once finished every block iteration and computation of all forces position, it is defined the linear programming problem [3] to evaluate the input smallest capacity C_M during and after block insertion as in Equation 1. If the minimum capacity during and after block placement are positive, we can conclude that the input block model is assemblable.

$$\underset{C_M, C_i, f_{f_i}, \mathbf{F}, \mathbf{F}_k, a_k}{\text{maximize}} \quad C_M \tag{1}$$

$$\text{subject to} \begin{cases} C_M \leq C_i = T - f_{f_i} & (i = 1, 2, \cdots, m) \\ \mathbf{W}_j \mathbf{A} \mathbf{F} = \mathbf{Q}_j & (j = 1, 2, \cdots, B) \\ \mathbf{F} = (\mathbf{F}_1^T, \cdots, \mathbf{F}_n^T)^T & \\ \mathbf{F}_k = \begin{cases} a_k \mathbf{t}_k & (k \in \mathcal{F}_f) \\ a_k \mathbf{n}_k & (k \in \mathcal{F}_n) \end{cases} & (k = 1, 2, \ldots, n) \\ a_k \geq 0 & (k = 1, 2, \ldots, n) \\ f_{f_i} = \sum_{k \in \mathcal{F}_{f_i}} a_k & (i = 1, 2, \ldots, m), \end{cases}$$

where C_i is the i-th connection capacity; T is the maximum friction force a connection can have; f_{f_i} is the i-th connection resultant friction force; m is the number of connections; $\mathbf{W}_j \mathbf{A}$ and $\mathbf{Q}_j$ are the j-th block wrench matrix and the applied external wrench, respectively; B is the number of blocks; $\mathbf{F}$ is the force vector with every force in the model and n is the total number of forces; a_k is the k-th force magnitude; $\mathbf{t}_k$ and $\mathbf{n}_k$ are the unit tangential and normal forces of the k-th force, respectively; $\mathcal{F}_f$ and $\mathcal{F}_n$ are the sets of indexes of friction and normal forces, respectively.

3. Experimental Constants

The mechanical analysis also needs the definition of a few experimental values. Those are: the maximum friction force a connection can handle before snapping out, the mass of each type of block and the value of gravity. The later was defined as $g = 9.8 m/s^2$. For the masses, an experiment was done using a precision scale to weigh each available block. The results are in the Table 1. Unlike what was believed, a twice bigger block does not have twice the mass. So it is necessary to weigh each new block type.

An experiment as in Fig. 4 as done to calculate the maximum friction value. Using a setting like this

it was done a set of experiments varying the hanging mass weight, number of connection points, and block type.

An example of one experiment free body diagram can be seen in Fig. 5. Where m_b is the block weight, m_w is the hanging mass weight, $\vec{g}$ is the gravity, l is the lenght of one knob, $\vec{F_{f1}}$ and $\vec{F_{f1}}$ are the sum of friction forces that appear in that connection. It was assumed that the friction forces in each connection would have the same maximum value and, for each experiment, it is possible to calculate the equilibrium of torques to find that value.

If a setting is not stable, that is, in the experiment the block snapped out of the base, it is assumed that the calculated friction force is greater than the maximum possible. On the other hand, if the block does not snap out, it is considered that the value is lower than that maximum.

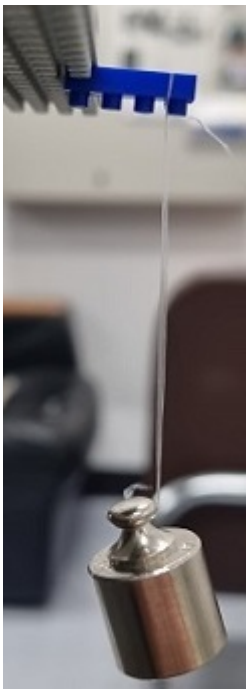

Fig. 4: Friction force experiment setup with one knob connected.

After the experiments it was found two different range of values for the maximum friction force. The first was found using 1 by N block types and it was between 150.788 and 175.458. The second using 2 by N block types was between 282.616 and 301.115. These values are in gram force. One possible explanation for distinct values range for this two types of blocks is the internal difference between them. The 2 by N internal structure provide less contact area than the 1 by N. As a conservative approach, it was used $151gf$ as the maximum force value in the algorithm.

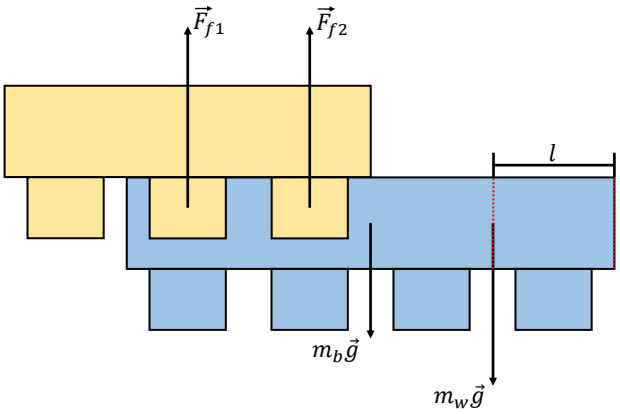

Fig. 5: Free body diagram for a 1 by 4 block experiment.

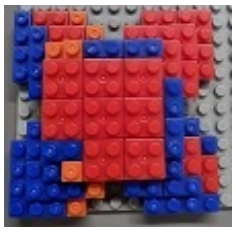

(a) Block model with only small block types.

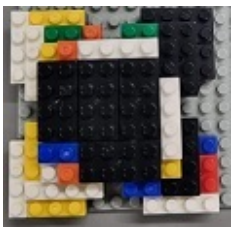

(b) Block model with any avail- able block types.

Fig. 6: Same input model assembled with different block types.

4. Results

To investigate the compatibility of the new strategy with the previous one, a set of block models using only the previously possible block types were used as input for both algorithms. The exact same C_m result was obtained for both, which suggests that they are compatible.

A complex input block model was created to investigate the impact of bigger block sizes in the 3D block printer usability. First it was executed utilizing only the three small block types previously possible. Then utilizing all available new block types. The assembled structure can be seen in Fig. 6(a) and Fig. 6(b).

The number of blocks was reduced from 104 in the first structure to 54. This reduction could be greater if more block types were available in the laboratory. The stability analysis gave both inputs the same output value, but, because the complexity of the algorithm is proportional to the number of blocks, the one using only the smaller bricks took 4.5 times more to finish execution.

5. Conclusion

To improve the previous 3D block printer, the previous mechanical analysis was restructured to allow the usage of more block types. Now it is possible

to use any 1 by N and 2 by N where $1 \leq N \leq 9$. Experiments was also done to define the value of experimental constants to elevate the reliability of the system output.

Those changes not only increase the range of possible objects that the 3D printer can assemble but also allows the same object to be built in less time and utilizing less material.

Further modifications are needed to utilize asymmetric blocks like the "L" and "T" shape types or the non-square blocks like the circular ones. It is also necessary to integrate the MATLAB mechanical analysis with the 3D block printer software in which assembly plans are generated to put these modifications into practical use.

References

[1] Stefanie Mueller, Tobias Mohr, Kerstin Guenther, Johannes Frohnhofen and Patrick Baudisch: "faBrickation: Fast 3D printing of functional objects by integrating construction kit building blocks," Proceedings of the SIGCHI Conference on Human Factors in Computing Systems, pp. 3827–3834, 2014.

[2] Mikiya Kohama, Chiharu Sugimoto, Ojiro Nakano and Yusuke Maeda: "Robotic additive manufacturing with toy blocks," IISE Transactions, Vol. 53, No. 3, pp. 273–284, 2020.

[3] Yusuke Maeda, Mikiya Kohama and Chiharu Sugimoto: "3D Block Printing: Additive Manufacturing by Assembly," IEEE/RSJ IROS 2019 Workshop on the current limits and potentials of autonomous assembly, 2019.

[4] Sheng-Jie Luo, Yonghao Yue, Chun-Kai Huang, Yu-Huan Chung, Sei Imai, Tomoyuki Nishita and Bing-Yu Chen: "Legolization: Optimizing LEGO designs," ACM Trans. on Graphics, Vol. 34, No. 6, pp. 1–222, 2015.